Results of laser-fusion experiments with the "Progress" facility and their interpretation

A. A. Andreev, M. G. Anuchin, V. G. Borodin, A. A. Gorokhov, A.L. Zapysov, A. I. Zuev, I. M. Izrailev, V. M. Komarov, V. G. Korolenko, V. B. Kryuchenkov, A. A. Mak, V. A. Malinov, V. M. Migel', N. V. Nikitin, V. A. Podgornov, V. G. Pokrovskiĭ, A. G. Samsonov, N. A. Solov'ev, V. A. Serebryakov, A. D. Starikov, A. V. Charukhchev, and V. N. Chernov

(Submitted 14 July 1988)
Zh. Eksp. Teor. Fiz. **95**, 528–536 (February 1989)

Results are reported of experiments on spherical irradiation of DT-gas-filled glass microspheres at a heating-radiation flux density $5 \cdot 10^{15}$ W/cm^2, performed with the "Progress" six-channel laser facility. The influence of the resonance mechanism on the efficiency of laser-energy absorption and on its transfer to the compressing shell is investigated. The experimental data are compared with computations by the "Zarya" and "Osvetka" codes and by a simple model of the interaction between the laser radiation and the shell. It is shown that the target-compression pattern depends strongly on the degree of development of the instabilities resulting from nonuniform irradiation of the targets.

1. INTRODUCTION

The main idea of laser fusion (LF) is to obtain high fuel density at temperatures that ensure an effective thermonuclear reaction. But there are serious difficulties in reaching and maintaining appreciable temperatures in the fuel, since the nonuniform target illumination and low precision with which the targets are produced leads to the onset of hydrodynamic instabilities.

We present here the results of experiments, performed with the six-channel "Progress" facility,[1] on the heating efficiency and compression stability of shell targets (glass microspheres). The experiments were performed at a radiation wavelength $\lambda = 1.06$ μm, power 0.5–1.0 TW, and pulse width at half maximum $\tau_{0.5} = 0.2$ ns. Six laser beams of diameter $2r_0 = 110$ mm were focused on the target with aspherical or three-lens objectives of focal length $F = 170$ mm (circles of least confusion 5–15 μm). The radiation power contrast was $\gtrsim 10^8$ at 1 ns before the pulse peak.[2]

In the experiments we irradiated glass microspheres filled with DT gas at up to 10–30 atm pressure. The target design was based on calculations by the "Zarya" code.[3] The parameters of the targets with the maximum neutron yield are well described by the following relation obtained for a simple model[4,5]:

$$R_0 = 700 \tau_{0,5}^{6/7} P_n^{2/7} / (\Delta R \lambda \rho_p)^{3/7}, \quad (1)$$

where R_0 and ΔR are the shell radius and thickness in μm, λ is in μm, $\tau_{0.5}$ is in ns, P_n is the absorbed power in TW, and ρ_p is the shell (pellet) density in g/cm.[3] Since technological considerations dictated $\Delta R \gtrsim 0.6$ μm, estimates in accordance with Eq. (1) yield in our case $R_0 \lesssim 75$ μm for a typical absorption coefficient $\sim 20\%$. We used in the experiments targets with $R_0 = 40$–75 μm and $\Delta R = 0.6$–1 μm; the target thickness varied by less than 5%. In a number of compression-stability experiments we used targets whose glass surfaces were coated with 0.1–0.6 μm of aluminum, and neon with pressure 2–4 atm was added in the shell to determine the degree of ablation.

The irregularity of the laser-radiation absorption over the target surfaces is one of the main causes of the onset of instability during compression. Absorption irregularity is due primarily to the dependence of the absorption on the angles at which the beam are incident on the target, and is determined by the geometry in which the rays are guided to the target; in our case this geometry differed somewhat from cubic.[6] The characteristic scales and amplitudes of the irregularities for various focusing errors d/R_0 of the objectives (d is the distance from the target center to the focus) were determined by computer calculations using the "Osvetka" program.[7] It was assumed that the laser radiation is absorbed by the inverse bremsstrahlung and resonance mechanisms. The calculations were performed in the geometric-optics approximation, with account taken of the beam refraction in the plasma. The radial profiles of the hydrodynamic parameters were calculated by the "Sfera" program[7] in the two-temperature hydrodynamics approximation. The energy input integrated over the beam trajectory was ascribed to the turning point. Calculations[7] have shown that the absorption irregularities have a characteristic scale 30–40 μm and an amplitude $\pm 20\%$ under typical experimental conditions ($2R_0 = 100$ μm, $d/R_0 = 3.2$). In addition to this large-scale irregularity, one of small scale (~ 10 μm) was produced in the experiments by modulating the intensity of each laser beam by $\pm 30\%$.

2. ABSORPTION AND CONVERSION OF LASER ENERGY

The laser energy absorbed by the target was measured by surrounding the target by plasma calorimeters of three types: differential,[8] calorimeters with a receiver element in the form of a dielectric mirror,[9] and calorimeters with a receiver element transparant to the laser radiation.[10] A group of five ion collectors was used to investigate the ion component of the plasma. The average ion charge was estimated by a procedure[10] based on comparing the readings of a plasma calorimeter and a collector for separate measurement of the charged-particle currents and the neutral-plasma-component energy. The electron temperature was determined with a seven-channel continuous x-ray spectrometer[11] at photon energies 4–43 keV, based on semiconductor and scintillator detectors with selective filters (absorption K-edges were used).

 0038-5646/89/020297-05$04.00

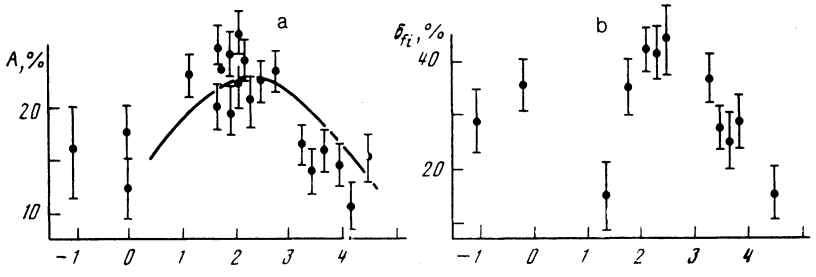

FIG. 1. Dependence of the absorption coefficient on d/R_0 (points—experiment, continuous curve—calculation by the "Osvetka" program) (a) and the ratio δ_{fi} of the fast-ion energy to the absorbed energy (b); laser irradiance $q = (1\text{–}2)\cdot 10^{15}$ W/cm^2.

To estimate the influence of various mechanisms on the laser-energy absorption we have investigated the dependence of the absorption coefficient, at laser-radiation flux densities $q = (1\text{–}2)\cdot 10^{15}$ W/cm^2 on the defocusing d/R_0 of the objectives relative to the target center (Fig. 1a). From a comparison with a theoretical curve calculated by the "Osvetka" program it can be seen that the experimental coefficient A is close to the calculated one. The absorption maximum is observed at $d/R_0 = 2.0\text{–}2.5$. Its appearance is due to the increase of the resonance absorption that depends on the angle of light incidence on the plasma. Starting from the results of Ref. 12, it can be shown that when the characteristic scale L_K of the plasma irregularity is determined by the radiation pressure the resonance absorption coefficient near the maximum is described by the expression

$$A_R = 0.35\sigma^2 \exp(-1.3\sigma^3). \qquad (2)$$

Here $\sigma = (r_0 d/2FR_{cr})(kL_{cr})^{1/3}$, $2r_0$ is the beam diameter on the focusing objective, F is the focal length of the objective, R_{cr} is the radius of the critical surface, $k = 2\pi/\lambda$, L_{cr} [in μm] $= 50T_c^{3/2}$ [in keV]/q [in units of 10^{14} W/cm^2],[13,14] and T_c is the thermal-electron temperature. Estimates based on Eq. (2), like calculations by the "Osvetka" program, yield $A_R \sim 10\%$, i.e., at $d/R_0 = 2\text{–}2.5$ and $q \sim 10^{15}$ W/cm^2 resonance absorption accounts for approximately 50% of the total absorbed energy.

The substantial role of the resonance absorption mechanism is confirmed also by the plot of $A(q)$, shown in Fig. 2 in the range $q = (0.1\text{–}6)\cdot 10^{15}$ W/cm^2 at two values of the defocusing d/R_0. The less steep decrease of the $A(q)$ curve for $q \geqslant 5\cdot 10^{14}$ W/cm^2 in the case $d/R_0 = 2.0\text{–}2.8$ can be attributed to an increase of the fraction of the resonantly absorbed energy, which balances the decrease of the classical bremsstrahlung absorption due to the increase of the slope of the plasma-density profile. The results can be approximated by the relation

$$A = A_0 q^{-\alpha}, \qquad (3)$$

where $A_0 = 0.54$, $\alpha = 0.5$ for $q = (0.1\text{–}2)\cdot 10^{15}$ W/cm^2, and $d/R_0 \geqslant 3$, while $A_0 = 0.35$, $\alpha = 0.25$ for $q = (0.5\text{–}6)\cdot 10^{15}$ W/cm^2 and $d/R_0 = 2.0\text{–}2.8$. Thus, the differences between the $A(q)$ dependences obtained for spherical targets irradiated in different laser facilities (see Ref. 15) can be attributed for the most part to different conditions of radiation focusing on the target and to the ensuing differences of the resonance-absorption contributions to the total absorption.

By increasing the energy input to the target, resonance absorption produces in the plasma a group of fast electrons that lose part of their energy to preheating the shell and the fuel, and give up the remaining part to the fast ions which they accelerate to $v_{fi} \geqslant 10^8$ cm/s. In the dependence of the absorbed-energy fraction δ_{fi} carried away from the plasma by the fast ions on the defocusing d/R_0 of the objectives (Fig. 1b), the maximum values $\delta_{fi} \sim 40\%$ were observed at the same $d/R_0 = 2.0\text{–}2.5$ as in the case when calculations show the resonance-absorption coefficient to be a maximum (Fig. 1a). The fast-electron temperature determined from the continuous x-ray spectrum and from ion measurements[10] increased from 6–8 keV for $d/R_0 > 3$ and $d/R_0 < 2$ to 15–20 keV for $d/R_0 = 2\text{–}3$. At the same time, the thermal-electron temperature depended little on d/R_0 and amounted to 0.8 ± 0.2 keV.

It must be noted that fast ions take practically no part in

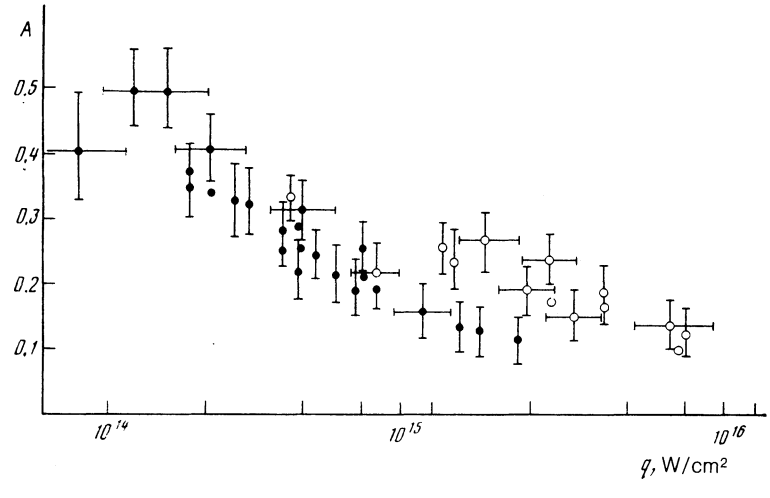

FIG. 2. Dependence of the absorption coefficient A on the laser-radiation flux density q for $d/R_0 = 2.0\text{–}2.8$ (○) and $d/R_0 \geqslant 3$ (●).

the ablation and heating of the fuel. In fact, since the shell-collapse rate is determined by the recoil momentum of the expanding plasma, the shell kinetic energy E_p can be represented in the form

$$E_p=2(E_T/c_s+E_{fi}/v_{fi})^2/M_p, \quad (4)$$

where E_T and E_{fi} are the total energies of the thermal and fast ions, c_s is the speed of the ion sound, and M_p is the shell mass. Since $c_s/v_{fi} \ll 1$, formation of fast ions does not increase the work performed by the ablation pressure.

3. DYNAMICS AND STABILITY OF TARGET COMPRESSION

Measurements of the time dependence of the plasma x rays, using vacuum x-ray diodes,[16] have made it possible to determine the average shell velocity v_e. This velocity is compared in Fig. 3 with the calculated velocity v_M obtained using the model of Refs. 4 and 5:

$$v_M=(R_0c_sc_T/3\Delta R)^{1/2}, \quad (5)$$

where $c_T = 5\cdot 10^6 P_n{}^{1/3} R_0{}^{-2/3}$ is the thermal-wave velocity in the solid target in cm/s, $c_s = 200\, c_T$, P_n is in TW, and R_0 and ΔR are in μm. It can be seen that, on the whole, the agreement between the calculation and the experiments is satisfactory, including experiments performed on other facilities.[16,17] At the same time, when fast-ion generation is appreciable ($\delta_{fi} \sim 40\%$) the shell velocity is significantly decreased by the decrease of the ablation pressure mentioned above.

One of the most important properties of the compression and heating of DT fuel is the neutron yield N, since it permits an estimate of the temperature T_i of the compressed DT gas. The yield N was measured by the delayed-registration method and by the time-of-flight method. The maximum yield N was $\sim 10^6$. Estimates of T_i were made with the aid of the relations given for T_i in Ref. 18, using the degrees of target compression obtained with x-ray pinhole cameras. In Fig. 4 the values of T_i obtained in this manner are compared with those computed by the "Zarya" program and using the model of Refs. 4 and 5. It can be seen that an increase of the specific energy input to the target, which is accompanied by an increase of the calculated T_i, does not increase the actual T_i of DT gas.

To ascertain the causes of these strong discrepancies between the computer calculations and experiment, we use the following relation of the model of Refs. 4 and 5:

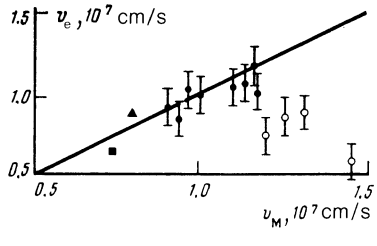

FIG. 3. Comparison of the experimental shell-collapse velocity v_e with the calculated velocity v_M obtained by the model of Refs. 4 and 5, for $\delta_{fi} \lesssim 20\%$ (●) and ~ 40 (○). The figure shows also data obtained with the "Sokol" (■)[16] and "Del'fin" (▲)[17] facilities.

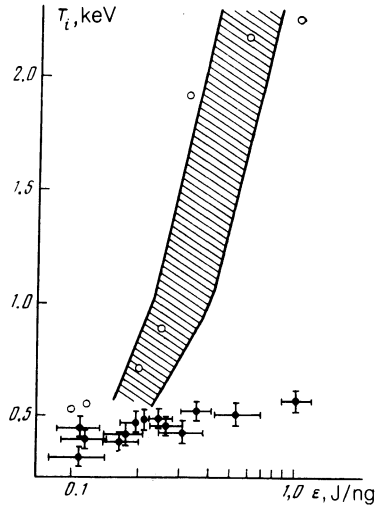

FIG. 4. Dependence of the ion temperature T_i of DT gas on the specific energy input ε(●). The shaded area covers the range calculations by the "Zarya" program, and the light circles denote values calculated by the model of Refs. 4 and 5.

$$T_i=6\cdot 10^6 \frac{c_T{}^2 v_M \tau_a}{\rho_0 R_0 + 50\,\Delta R}, \quad (6)$$

where T_i is in keV, c_T and v_M are in units of 10^7 cm/s, τ_a is the effective ablation-pressure action time in ns, R_0 and ΔR in μm, and ρ_0 is in mg/cm^3. It can be seen from (5) and (6) that T_i can be increased 1) by decreasing the shell thickness ΔR, 2) by decreasing the initial DT-gas density, and 3) by decreasing the absorbed power P_n. The first two procedures contribute to development of hydrodynamic instabilities in the course of shell compression, and for $q > 5\cdot 10^{14}$ W/cm^2 the third leads to formation of fast ions, and hence to lowering of the ablation pressure.

These conclusions are indirectly confirmed by the plot, shown in Fig. 5, of the ratio of the experimental neutron yield to the yield N_M calculated by the model of Refs. 4 and 5 from the final degree δ of the fuel bulk compression determined from x-ray pinhole photographs for different δ_{fi}. The reduction of N_e/N_M for $\delta > 200$ and for small $\delta_{fi} \lesssim 20\%$ is apparently due mainly to development of hydrodynamic instabilities. If, however, the fast ions carry away a significant fraction of the absorbed energy ($\delta_{fi} \sim 40\%$), the neutron yield becomes much lower than the calculated value even for small compressions $\delta \sim 100$–200, owing to the decrease of the ablation pressure, a result that correlates with the decrease of the shell-collapse rate (Fig. 3).

The substantial influence of the hydrodynamic instabilities on the target-compression process is confirmed directly by our experiment with two-layer ($Al + SiO_2$) shells[18] and with Ne added to the DT gas.[19] Spectroscopic investigations of the spatial brightness distributions in the Si and Al lines have shown that the intense regions of these lines for the compressed part of the target were equal in a number of experiments. Yet one-dimensional computations by the "Zarya" program indicated an absence of aluminum from the compressed part of the shell. Investigations of the DT-gas pressure by measuring the Ne line brightness have shown that the degree of compression can be ~ 4 times smaller than calculated.

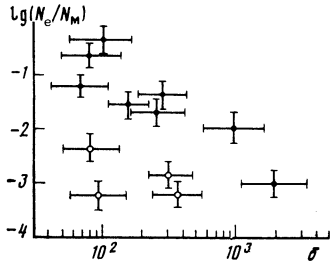

FIG. 5. Ratio of experimental neutron yield N_e to the yield N_M calculated by the model of Refs. 4 and 5 vs the final stage of the bulk compression δ for $\delta_{fi} \leqslant 20\%$ (○) and $\sim 40\%$ (●).

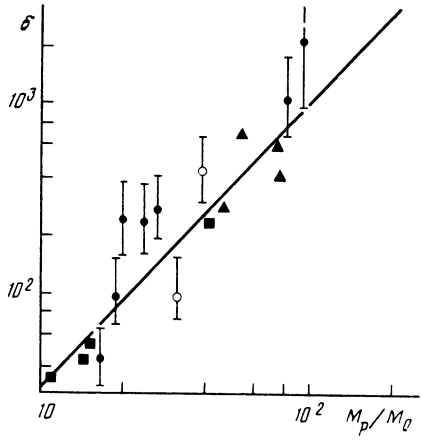

FIG. 7. Degree of bulk compression δ vs the ratio of the shell mass M_p to the gas mass M_0 at $\delta_{fi} \lesssim 20\%$ (●) and $\delta_{fi} = 40\%$ (○): solid line—plot of $\delta = (M_p/M_0)^{3/2}$. Data obtained with the "Del'fin"[17] (▲) and "Iskra"[22] (■) facilities are shown for comparison.

The dimensions of the region where the shell and the DT gas are mixed can be estimated from the following considerations. The small-scale variation of the target illumination, enhanced by self-focusing in the plasma corona, produces in the absorption region "hot" spots that are transferred to the ablation zone and initiate the development of Rayleigh–Taylor instabilities during the collapse state, the perturbations with the largest growth rate being those having transverse dimensions $\sim 10\,\mu$m.[20] During the linear stage of instability development, the growth rate is appreciable,

$$\varkappa = \frac{1}{2}\left(\frac{R_0}{\Delta R}\right)^{1/2} \int_{0,25}^{1} \left\{ -\frac{d}{dx} \right.$$

$$\times \left. \ln\left[\frac{4}{3}\beta(1-x^2)\right]^{1/2} \right\}^{1/2} dx \approx 5. \qquad (7)$$

where $\beta = R_0 c_T / c_s \Delta R$, $x = R/R_0$. The nonlinear hydrodynamic-instability stage that evolves in our case apparently gives rise to turbulent mixing of the shell and a gas over a length[21] L given by

$$L = 270\beta_1^4 \ln(\rho_p/\rho_0) R_0 \int_{x_k}^{0,25} \left(-\frac{d}{dx} \ln V \right)^{1/2} dx, \qquad (8)$$

where $\beta_1 = 0.133$, $x_k = \delta^{1/3}$, ρ_p and ρ_0 are respectively the shell and gas densities,

$$V^2(x) = (4\beta/3)(1 - x_k^2/x^2)/(1 - 16x_k^2).$$

One-dimensional computer calculations show that $\rho_p/\rho_0 \sim 10$ and consequently $L \sim 0.1R_0$ during the $x < 0.25$ stage, when the DT gas produces a backpressure. A region with characteristic length $L \sim 0.1R_0$ in which the gas is mixed with the shell material can be produced in the experiment. This should lower the temperature of the compressed DT and the neutron yield.

At the same time, pinhole photographs of the compressed target show that during the final stage the shell glow is annular (Fig. 6). The degrees of bulk compression obtained from the pinhole photographs agree well with those computed by the "Zarya" program.[19] This indicates that the pellet collapses as a unit, and the perturbations caused by the electrodynamic instabilities penetrate into the compressed DT gas in the form of "tongues" and basically lower its final temperature. The degree of bulk compression δ determined from the pinhole photographs is thus an upper bound of the true compression.

Figure 7 shows the dependence of δ on the ratio of the shell mass M_p to the gas mass M_0, together with data obtained from other facilities.[17,22] Clearly, this dependence is well described by the relation obtained in the model of Refs. 4 and 5:

$$\delta = (M_p/M_0)^{3/2}. \qquad (9)$$

It is clear from Fig. 7 that even when an appreciable number of fast ions is generated ($\delta_{fi} \sim 40\%$) the value of δ

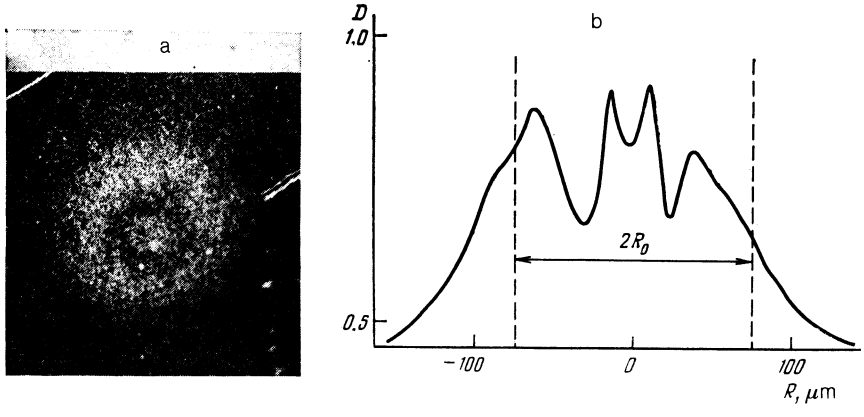

FIG. 6. a) Pinhole x-ray photograph of a target at photon energies 2.5 keV. b) Corresponding density pattern.

decreases insignificantly (by not more than a factor of 2). This allows us to estimate the influence of the fast electrons on the preheating of the DT gas. Let the total energy of the fast electrons entering the target be E_{fe}; the energy fraction remaining in the gas and heating it prior to the arrival of the shock wave is equal to $E_{fe}(M_0/M_p)$. Using arguments similar to those in Refs. 4 and 5 we obtain the following expression for the degree of gas compression, with allowance for preheating by the fast electrons:

$$\delta = \left[\frac{M_p}{M_0} \Big/ (1+\alpha E_{fe}/E_k)\right]^{3/2}, \qquad (10)$$

where E_k is the kinetic energy of the collapsing shell and $\alpha \lesssim 1$. Estimates of E_k, based on measurements of the collapse rate (Fig. 3), yield $E_k/E_a \approx 1$–3%, where E_a is the absorbed energy. From this, recognizing that the degree of compression is lowered by the fast electrons by no more than a factor of 2, we find on the basis of Eq. (10) that the energy lost by the fast electrons in the shell and in the gas is 0.5–2.0% of the absorbed energy. Thus, the fast electron produced in resonance absorption lose their energy mainly to fast-ion acceleration and not to gas preheating. The gas preheating by the electrons, even for $q \geqslant 10^{15}$ W/cm^2, does not exceed the preheating by the shock wave produced by the moving shell.

4. CONCLUSION

Let us formulate briefly the main distinctive features of the interaction between high-power laser radiation ($q \sim 10^{15}$ W/cm^2, $\tau_{0.5} = 0.2$ ns) with spherical glass targets of 80–150 μm diameter and wall thickness 1.0 μm, filled with DT gas to pressures up to 10–30 atm.

The laser radiation is absorbed in the target corona with efficiency $\lesssim 25\%$, depending on the defocusing of the objectives relative to the target center. An appreciable part, $\sim 40\%$, of the total absorbed energy is captured by the resonance mechanism and is transferred to the resulting fast electrons. The fast electrons leave the plasma and transfer the bulk of their energy to the fast ions. The fast ions do not contribute to the ablation pressure, and their energy is uselessly lost, decreasing thereby the rate of shell collapse and the DT-gas temperature. No more than 2% of the absorbed energy goes into fast electrons that preheat the shell and the gas, and the preheating of the gas by the fast electrons is less than the preheating by the shock wave produced by the moving shell. The ablation pressure produced by the thermal ions accelerates the shell inward and compresses it as a unit. However, the perturbations produced by the small-scale inhomogeneity of the illumination and building up as a result of hydrodynamic perturbations lower the final DT-gas temperature. This prevents simultaneous attainment of high DT-gas densities and temperatures at compressions > 100.

[1] V. N. Alekseev, E. G. Bordachev, V. G. Boronin *et al.*, Izv. AN SSSR, Ser. Fiz. **48**, 1477 (1984).
[2] V. I. Kryzhanovskiĭ, A. A. Chertkov, V. A. Malinov *et al.*, Kvant. Elektron. (Moscow) **12**, 372 (1985) [Sov. J. Quant. Electron. **15**, 239 (1985).
[3] E. N. Avrorin, A. I. Zuev, N. E. Karlykhanov *et al.*, IPM Preprint No. 77, Inst. Appl. Math., Moscow, 1980.
[4] A. A. Andreev, A. A. Mak, V. A. Serebryakov, and I. A. Solov'ev, Izv. AN SSSR, Ser. Fiz. **48**, 2270 (1984).
[5] A. A. Andreev and I. A. Solov'ev, Kvant. Elektron. (Moscow) **12**, 851 (1985) [Sov. J. Quant. Electron. **15**, 556 (1985)].
[6] A. A. Andreev, A. A. Gorokhov, A. B. Mikhaĭlov *et al.*, Opt. Spektrosk. **59**, 847 (1985) [Opt. Spectrosc. (USSR) **59**, 511 (1985)].
[7] A. A. Andreev, A. A. Gorokhov, A. A. Mak *et al.*, Abstracts, All-Union Seminar on the Physics of Rapid Processes in a Plasma, Grodno, Grodno State Univ. Press, 1986, p. 17; A. A. Andreev, A. G. Samsonov, and I. A. Solov'ev, Kvant. Elektron. (Moscow) **14**, 1873 (1987) [Sov. J. Quant. Electron. **17**, 1195 (1987)].
[8] S. R. Gunn and V. C. Rupert, Rev. Sci. Instr. **48**, 1375 (1977).
[9] V. M. Komarov, A. V. Mezenov, V. M. Migel', and N. V. Ponomarev, Prib. Tekh. Eksp. No. 2, 210 (1987).
[10] A. A. Andreev, V. M. Komarov, and A. G. Samsonov, Abstracts, All-Union Seminar on the Physics of Rapid Processes in a Plasma, Grodno, Grodno State Univ. Press, 1986, p. 14.
[11] A. S. Ganeev, A. L. Zapysov, A. I. Zuev *et al.*, Kvant. Elektron. (Moscow) **9**, 711 (1982) [Sov. J. Quant. Electron. **12**, 439 (1982)].
[12] A. A. Andreev, V. I. Kryzhanovskiĭ, and N. A. Solov'ev, Opt. Spektrosk. **54**, 577 (1983) [Opt. Spectrosc. (USSR) **54**, 343 (1983)].
[13] D. T. Attwood, IEEE J. **QE-14**, 909 (1978).
[14] K. Estabrook and W. L. Kruer, Phys. Rev. Lett. **40**, 42 (1978).
[15] N. G. Basov, Yu. A. Zakharenkov, N. N. Zorev *et al.*, Itogi Nauki i Tekhniki, Radiotekhnika, VINITI, Moscow, Vol. 26, Part 1, 1982.
[16] V. Volenko, A. F. Ivanov, L. A. Malitsin *et al.*, Pis'ma Zh. Eksp. Teor. Fiz. **37**, 328 (1983) [JETP Lett. **37**, 389 (1983)].
[17] I. V. Aleksandrova, N. G. Basov, B. L. Vasin *et al.*, Kvant. Elektron. (Moscow) **10**, 1677 (1983) [Sov. J. Quant. Electron. **13**, 1103 (1983)].
[18] N. M. Barysheva, A. A. Gorokhov, A. A. Zapysov *et al.*, *ibid.* **13**, 873 (1986) [**16**, 543 (1986)].
[19] M. G. Anuchin, V. G. Borodin, A. A. Gorokhov *et al.*, Pis'ma Zh. Eksp. Teor. Fiz. **44**, 71 (1986) [JETP Lett. **44**, 88 (1986)].
[20] J. Nuckols, L. Wood, A. Thyssen, and G. Zimmermann, Laser-Fusion Problems [Russ. transl.], Atomizdat, 1976, p. 27.
[21] S. Z. Belen'kiĭ and E. S. Fradkin, Trudy FIAN **29**, 207 (1965).
[22] E. N. Avrorin, V. A. Eroshenko, A. I. Zaretskiĭ *et al.*, Zh. Eksp. Teor. Fiz. **87**, 417 (1984) [Sov. Phys. JETP **60**, 239 (1984)].

Translated by J. G. Adashko